Comprehensive Journal of Science
Volume (11), Issue (42), (Sapt, 2026)
ISSN: 3104-6266

مجلة العلوم الشاملة
المجلد (11) العدد 42 سبتمبر 2026
ردمد: 3104-6266

Design and Performance Analysis of an Off-Grid Rooftop PV System in Zintan, Libya

*Saleh A. Almajdup [1 *], Asmail Alfrjani Alshanta [2], Omar K. Fernan [3]*
[1.2.3] the Mechanical Engineering Department at the Higher Institute of Science and Technology in Zintan, Libya,
[*]Corresponding author: s.almajdup@gmail.com

Received: 12/10/2026 Revised: 15/10/2026 Accepted: 02/11/2026 Publication: 21/11/2026

Abstract:
This study presents a comprehensive engineering design, dynamic modeling, and performance evaluation of a standalone (off-grid) rooftop solar photovoltaic (PV) system, integrated with an AGM lead-acid battery bank and a backup diesel generator. The system is designed to meet the daily energy requirements of the Mechanical Engineering Department at the Higher Institute of Science and Technology in Zintan, Libya. Sizing criteria were based on the most restrictive mathematical constraints of the winter season to safeguard critical infrastructure against national grid instability and frequent outages. Long-term modeling was conducted using PVsyst at an hourly temporal resolution. The optimal system configuration consists of an 11.44 kWp monocrystalline solar PV array, coupled with a lead-acid battery storage system (AGM type, 48V, 1176 Ah—equivalent to 59.4 kWh nominal energy), and a 12 kW smart backup generator. The annual simulation report indicates a robust Performance Ratio (PR) of 69.36% and an exceptional Solar Fraction (SF) of 90.95%, with the solar array generating 19,547 kWh of usable energy annually. The backup generator operates automatically based on a strict dual-threshold logic tied to the battery State of Charge (SOC), consuming 235 liters of diesel per year to supply 1,760 kWh/year. These results demonstrate that this optimized, autonomous system effectively ensures absolute power reliability, protects sensitive laboratory equipment, and maintains a high battery State of Health (SOH) of 97.4% after one year of operation, confirming its technical, economic, and environmental viability.

Keywords: Off-grid PV, PVsyst, backup generator, national grid instability, storage system**.**

تصميم وتحليل أداء نظام طاقة شمسية كهروضوئية مستقل فوق الأسطح بمدينة الزنتان، ليبيا

صالح ابوراوي المجدوب[1 *]، إسماعيل الفرجاني الشنطة [2]، عمرخليفة فرنانة [3]
[1.2.3] قسم الهندسة الميكانيكية بالمعهد العالي للعلوم والتقنية في الزنتان، ليبيا.

الملخص
تقدم هذه الدراسة تصميماً هندسياً شاملاً، ونمذجة ديناميكية، وتقييماً للأداء لنظام طاقة شمسية كهروضوئية (PV) مستقل (غير متصل بالشبكة) مُركَّب على سطح مبنى، ومدمج مع مجموعة بطاريات حمضية من نوع (AGM) ومولد ديزل احتياطي. صُمم النظام لتلبية الاحتياجات اليومية من الطاقة لقسم الهندسة الميكانيكية في المعهد العالي للعلوم والتقنية في مدينة الزنتان بليبيا. وقد استندت معايير تحديد حجم المكونات إلى أكثر القيود الرياضية صرامةً خلال فصل الشتاء، وذلك لضمان حماية البنية التحتية الحيوية في ظل عدم استقرار الشبكة الوطنية وتكرار انقطاعات التيار الكهربائي. أُجريت النمذجة طويلة المدى باستخدام برنامج (PVsyst) بدقة زمنية تعتمد على فترات hourly (ساعة بساعة). يتكون التكوين الأمثل للنظام من مصفوفة ألواح شمسية أحادية البلورة (monocrystalline) بقدرة 11,44 كيلوواط ذروة (kWp)، مقترنة بنظام تخزين يعتمد على بطاريات حمضية (من نوع AGM، بجهد 48 فولت وسعة 1176 أمبير-ساعة، أي ما يعادل طاقة اسمية قدرها 59,4 كيلوواط-ساعة)، بالإضافة إلى مولد احتياطي ذكي بقدرة 12 كيلوواط. يشير تقرير المحاكاة السنوي إلى تحقيق "معامل أداء" (Performance Ratio - PR) قوي بنسبة 69,36%، و"نسبة مساهمة شمسية" (Solar Fraction - SF) استثنائية بلغت 90,95 %، حيث تولد المصفوفة الشمسية 19,547 كيلوواط-ساعة من الطاقة القابلة للاستخدام سنوياً. يعمل المولد الاحتياطي تلقائياً وفق منطق دقيق

يعتمد على عتبتين مرتبطتين بـ "حالة شحن البطارية" (State of Charge - SOC)، حيث يستهلك 235 لتراً من الديزل سنوياً لتوفير 1,760 كيلوواط-ساعة. وتُظهر هذه النتائج أن هذا النظام المستقل والمُحسَّن يضمن موثوقية عالية جداً في إمدادات الطاقة، ويحمي المعدات المختبرية الحساسة، كما يحافظ على "حالة صحة البطارية" (State of Health - SOH) عند مستوى مرتفع يبلغ 97,4 % بعد عام واحد من التشغيل؛ مما يؤكد جدواه من النواحي التقنية والاقتصادية والبيئية.

الكلمات المفتاحية: أنظمة الطاقة الكهروضوئية المستقلة (خارج الشبكة)، برنامج PVsyst، مولد احتياطي، عدم استقرار الشبكة الوطنية، نظام تخزين

1. Introduction

The sun provides the fundamental energy that sustains life on Earth; in just one hour, the planet receives enough solar energy to meet global demand for nearly a full year [1]. Solar energy has emerged as a crucial renewable energy source, playing a pivotal role in offering the clean solutions required for sustainable development [2]. Over the past decade, Libya's renewable energy sector has planned numerous utility-scale and decentralized projects, primarily leveraging solar and wind resources as the two most viable alternatives for the country. Libya experiences an average solar radiation of approximately 7.5 kWh/m²/day, with 3,000 to 3,500 hours of sunshine annually, making its solar resource wealth among the highest in the world with an annual horizontal average exceeding 2,200 kWh/m² [3]. Concurrently, average wind speeds range from 6 to 7.5 m/s at a reference height of 40 meters [4]. These vast renewable assets, distributed across an area of 1,750,000 square kilometers, could completely satisfy Libya's domestic electricity needs, support neighboring regional networks, and enable clean power export to Europe via High-Voltage Direct Current (HVDC) transmission frameworks [5]. Regarding rural electrification and isolated load management, solar photovoltaic (PV) technology has become the preferred choice due to its high modular versatility, allowing systems to be tailored precisely to remote, off-grid architectures. While classical engineering relied on simple, static rules for sizing standalone PV systems, modern smart controllers enable highly dynamic, integrated management. Off-grid system configurations range from elementary DC-coupled layouts to complex, multi-source hybrid microgrids, dictated by power demands, inductive load characteristics, localized meteorological profiles, and economic constraints [6]. Photovoltaic arrays generate electricity in a clean, silent, and highly reliable manner [7]. Individual PV cells are interconnected into weather-resistant modules, which are further combined in series and parallel topologies to meet specific voltage and current thresholds [8]. The rigorous design of a PV energy system requires meticulous component selection and sizing tailored to geographical and load parameters [9]. Advanced simulation tools, such as PVsyst, are required to analyze non-linear operational parameters, near-shading behaviors, temperature coefficients, and spectral shifts. In comparison, standard tools like HOMER present limitations; they do not generate current-voltage (I-V) curves, fail to conduct multi-variable near-shading geometric analyses, restrict meteorological data imports from custom or localized ground stations, and omit several thermodynamic array loss paths, making them less ideal for comprehensive engineering validation [10].

This study presents a real-world engineering case study on the sizing, optimization, and validation of an autonomous rooftop solar PV microgrid for the Mechanical Engineering Department at the Higher Institute of Science and Technology in Zintan, Libya. The analysis evaluates the performance of the system by cross-referencing mathematical formulations with dynamic hourly simulation metrics generated via the PVsyst engine.

2. SITE SURVEY

2.1 Geographical and Administrative Overview

The Zintan region is a strategically vital area located in northwestern Libya at a latitude of 31.93056° N and a longitude of 12.24833° E, operating within the UTC+2 time zone [12]. The city is situated atop the Nafusa Mountain plateau at an elevated altitude ranging between 650 and 710 meters above sea level, approximately 136 kilometers southwest of the capital, Tripoli as shown in Figure 1 [13]. High-altitude environments directly enhance PV conversion parameters; the lower average ambient temperatures mitigate the severe thermal voltage degradation typical of low-altitude desert environments, providing a higher overall annual Performance Ratio (PR) [15].



Figure 1: Geographical Map and Location Profile of Zintan.

2.2 Population and Demographics

According to the last national census executed by the Libyan Bureau of Statistics and Census in 2006, the total population of the Zintan Municipality encompassed approximately 62,000 residents [11]. Subsequent international demographic tracking estimated the dense urbanized core at approximately 16,024 residents [11, 14]. Due to regional geopolitical instability post-2011, no official nationwide census has been completed, leaving the 2006 census as the baseline statistical authority [11].

2.3 Solar Radiation, Temperature, and Meteorological Profile

Zintan possesses an exceptionally high potential for solar energy harvesting [12, 14]. Its high elevation significantly reduces atmospheric attenuation, granting it crisp, clear sky conditions for most of the year [12]. The area transitions between a Mediterranean climate and a semi-arid desert climate, rendering high annual solar irradiance across all seasons alongside a distinct ambient temperature profile that closely dictates PV conversion efficiencies [12, 14]. Table 1 presents the average annual solar radiation, temperature, and meteorological measurements for the Zintan region.

Table 1: Annual solar radiation, temperature, and meteorological metrics for the Zintan region.

Solar / Meteorological Metric	Value / Quantity
Annual Avg. Horizontal Irradiance (GHI)	5.8 – 7.2 kWh/m²/day [12]
Peak Season (July Max Avg.)	8.2 kWh/m²/day [12]
Low Season (December Min Avg.)	3.2 kWh/m²/day [12]
Average Daily Sunshine Hours	9.5 – 10.5 hours/day [12]
Average Ambient Temperature Range	1°C (Winter Min) – 38°C (Summer Max) [12]
Optimum PV Tilt Angle (Annual Fix)	28° – 30° South [12], [14]

The annual average Global Horizontal Irradiance (GHI) for Zintan establishes a robust baseline for year-round power production. During the peak summer season in July, the maximum average irradiance reaches 8.2 kWh/m²/day, coinciding with ambient peak temperatures ranging between 32°C and 38°C (with absolute maximums exceeding 40°C). This extreme solar surge maps perfectly onto peak domestic cooling demands and high regional grid loads. However, standard silicon PV modules experience a negative thermal efficiency degradation coefficient ranging from -0.35% to -0.45% per degree Celsius above 25°C. The high ambient summer temperature causes the cell operating temperature to climb significantly, inducing a temporary drop in instantaneous efficiency due to thermal voltage degradation [11], [13].

Conversely, the low season in December exhibits a minimum average irradiance of 3.2 kWh/m²/day, which serves as the critical mathematical boundary condition for sizing autonomous energy storage systems (Off-Grid Battery Banks). Interestingly, winter ambient temperatures in Zintan drop significantly, ranging from 1°C to 14°C. This pronounced winter cooling acts as a substantial physical asset, lowering cell operating temperatures, increasing semiconductor conductivity, and boosting the open-circuit voltage (Voc). This natural thermal optimization effectively compensates for the shorter winter daylight hours and intermittent cloud cover [12], [13].

The region benefits from an extensive average daily sunshine duration of 9.5 to 10.5 hours/day [12]. This stable daylight window minimizes rapid input power ramping fluctuations, thereby preventing premature thermal fatigue on digital inverter units. To maximize cumulative annual kilowatt-hour yields without incurring the capital costs and maintenance overhead of active mechanical tracking units, the optimum fixed geometric photovoltaic tilt angle is determined to be 28° – 30° oriented due South [12], [14]. Furthermore, the mountain terrain promotes natural convective air currents that assist in cooling the arrays, provided an engineered air gap of 15–20 cm is maintained beneath the substructure to facilitate continuous airflow [13].

The following graph, Figure 2, illustrates the seasonal performance curve, which models the interplay between Global Horizontal Irradiance (GHI) and ambient temperature fluctuations throughout the year in the city of Zintan

This curve clearly demonstrates the seasonal correlation, tracing the transition from the cold winter months—characterized by low solar irradianceto the peak of summer, which is marked by high temperatures and maximum levels of solar radiation.

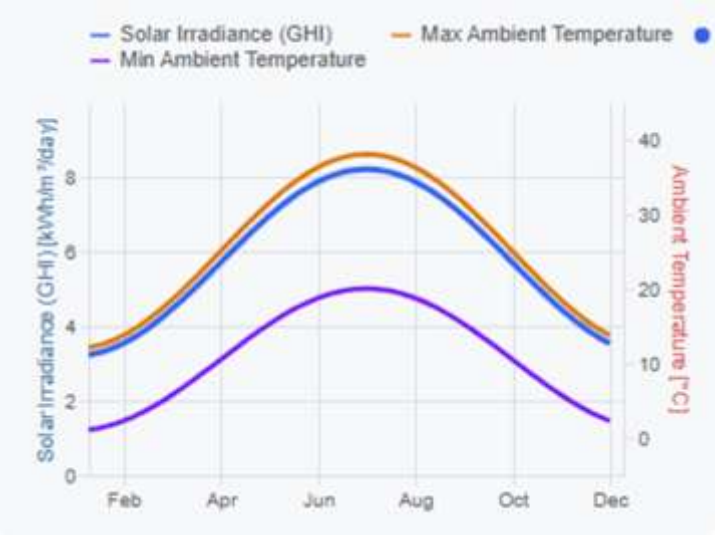


Fig. 2 Seasonal thermal-solar correlation [16], [19].

Furthermore, Figure 3 clearly shows that the peak solar radiation (8.2 kWh/m²/day) coincides with the highest summer temperatures (38°C) in July, highlighting the significant thermal stress photovoltaic cells endure. Conversely, the lower levels recorded in December (3.2 kWh/m²/day) coincide with lower ambient temperatures (1°C), which helps maximize the voltage efficiency of the semiconductors.

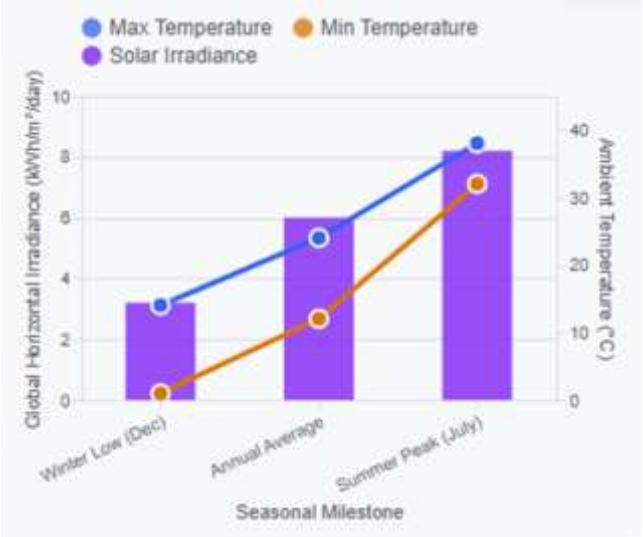


Fig. 3. Discrete Seasonal Performance Milestones [16], [17].

3. PROBLEM STATEMENT

The energy landscape in Libya, particularly in high-altitude regions like Zintan, presents critical operational, infrastructural, and environmental challenges that heavily disrupt educational frameworks:

• Severe Grid Instability: The Libyan national electricity network experiences massive supply deficits, localized overloads, and chronic load-shedding, resulting in sudden, prolonged blackouts.

• Appliance Vulnerability: Frequent, unmetered voltage fluctuations and grid shocks cause severe electronic component failures and permanent damage to expensive, sensitive laboratory equipment.
• Intermittency and Storage Overhead: Shifting to decentralized solar energy introduces seasonal generation intermittency, requiring precise technical balancing to prevent system under-sizing during winter overcast periods.
• Environmental Strain: Localized reliance on fossil-fuel backup configurations (unregulated diesel generators) induces severe localized greenhouse gas emissions and public health hazards.

4. PROPOSED TECHNICAL SOLUTIONS AND CONTRIBUTIONS

To address these formidable challenges, this study proposes a comprehensive technical solution through the design of an autonomous rooftop solar PV system for the Mechanical Engineering Department building at the Higher Institute of Science and Technology in Zintan, Libya. The specific contributions and solutions are outlined below:

4.1 Overcoming Generation Intermittency: Integrating an optimized Standalone PV system with AGM energy storage to capture excess solar power during peak daylight hours, ensuring continuous load coverage during non-generation periods and weather fluctuations.

4.2 Mitigating National Grid Unreliability: Addressing the unreliability of the national electrical grid: providing a fully independent power source for the educational institution, thereby ensuring that critical school facilities—such as laboratories, classrooms, and servers—are protected from frequent power outages, load-shedding, and voltage instability within the national grid.

4.3 Countering Aging Plant Deficits via Critical Sizing: Engineering the system sizing metrics based on the absolute worst-case winter scenario in Zintan (3.2 kWh/m²/day in December), guaranteeing that the school's electricity needs are met even during prolonged winter overcast days.

4.4 Preventing Consumer Load and Appliance Damage: Utilizing high-tier digital inverters and charge controllers to deliver clean, stabilized Alternating Current (AC) electricity, which eliminates the risk of equipment failure caused by national grid electrical shocks.

4.5 Eliminating Environmental Emissions and Health Hazards: Replacing fossil-fuel dependency (oil and gas) with a zero-emission rooftop solar installation directly reduces greenhouse gases, combats climate change, and promotes a healthier environment for the community.

5. OBJECTIVES OF THE STUDY

The primary goal of this research is to design, validate, and optimize an autonomous off-grid rooftop solar PV microgrid for the Mechanical Engineering Department at Zintan, ensuring zero-loss load coverage. The specific research objectives are:
1. Resource Assessment: Evaluate localized high-altitude meteorological profiles (average Global Horizontal Irradiance and temperature thresholds) using Metronome 9.0 database.
2. Critical-Month Sizing: Size the optimal cross-sectional capacities of the PV matrix and battery bank based on the worst-case winter design boundary conditions (3.2 kWh/m²/day in December).
3. Thermal Power Mitigation: Analyze the non-linear impact of ambient summer temperatures on voltage degradation to specify passive air-gap cooling constraints.
4. Hybrid Microgrid Integration: Optimize an automated dual-threshold SOC dispatch logic for a 12-kW backup generator to minimize fuel consumption while maintaining battery durability.
5. Analytical Validation: Perform a rigorous validation matrix comparing theoretical analytical

hand formulations against dynamic hourly software simulations via PVsyst.
6. Ecological Impact Quantification: Calculate the annual and life-cycle greenhouse gas emission offsets achieved by replacing fossil-fuel dependencies with zero-emission technology.

6. RESEARCH METHODOLOGY, MATHEMATICAL VALIDATION, AND SIMULATION RESULTS

6.1 Geographical Site and Case Study Description

To address issues related to the stability of the electrical grid in Libya, this paper proposes a standalone, photovoltaic-powered microgrid system, located at the Mechanical Engineering Department building of the Higher Institute for Science and Technology in Zintan, Libya. Geographically, the facility is situated at a latitude of 31.9280° N, a longitude of 12.2507° E, and an elevation of 694 meters above sea level (within the UTC+2 time zone). This elevation provides excellent clear-sky conditions, which minimize atmospheric attenuation—the loss of energy caused by the atmosphere—for the majority of the year. The study utilizes environmental and meteorological parameters derived from the "Meteonorm 9.0" database. The available installation area on the building's rooftop, shown in Figure 4 below, consists of a flat surface of approximately 200 square meters; this imposes constraints on the layout of the solar panels and necessitates careful planning to avoid any shading.



Figure 4. The Higher Institute of Science and Technology in Zintan, Libya

6.2 Electrical Demand & Daily Load Profile

he autonomous infrastructure is engineered around the actual daily operational profile of the mechanical department. The facility operates on a standard 6 days per week institutional routine with a simulated baseline benchmark of 54 kWh/Day. The cumulative daily energy requirement calculated across all academic assets stands at 62,484 Wh/day (62.48 kWh/day) with a total peak connected load of 9.50 kW [21]. The electrical appliances, along with their power ratings and daily operating durations, are outlined in Table 2 below.

Table 2: Load Data and Daily Energy Consumption Of Mechanical Engineering Department.

Appliance Category	Qty	Unit Rating (W) & Use Profile	Daily Energy (Wh/Day)
Lamps (LED)	27	20 W per lamp / 8.0 Hours/day	4,320
Security Cameras	6	10 W per app / 24.0 Hours/day	1,440
Laboratory Printers	2	500 W per app / 2.0 Hours/day	2,000
Fridge / Deep-freeze	1	18.0 Hours/day continuous operational cycle	3,600
Air Conditioners	4	8.0 Hours/day simultaneous cooling cycle	48,000
Computers	2	200 W combined asset total / 4.0 Hours/day	1,600
Water Pump	1	1500 W independent system / 1.0 Hours/day	1,500
Stand-by Base Loads	—	24.0 Hours continuous leakage baseline	24
Cumulative Total Load	**—**	**Daily Calculated Institutional Total**	**62,484**

The electrical appliances, along with their power ratings and daily operating durations, are outlined in Table 2. The dynamic chronological distribution of this electrical demand across a 24-hour cycle is simulated via PVsyst and illustrated in Figure 5.

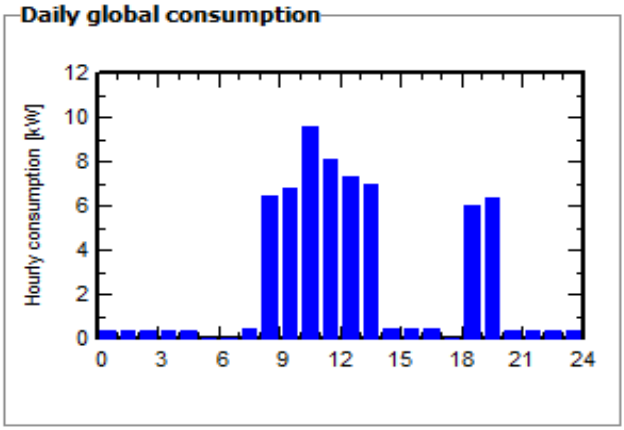


Figure 5: Hourly electrical consumption of the department

As explicitly shown in Figure 5, the load profile displays a sharp increase beginning at 08:00 due to classroom activation and the heavy inductive demand of the 4 air conditioning units (48 kWh/day). The simulated curve demonstrates that the load profile reaches its absolute maximum peak capacity of 9.50 kW between 11:00 and 14:00, aligning perfectly with peak localized solar irradiance hours. After 14:00, the consumption decreases dynamically, returning to an overnight base load profile of approximately 1,440 Wh/day dedicated strictly to security cameras and baseline IT infrastructure." [21].

As explicitly shown in Figure 5, the load profile displays a sharp increase beginning at 08:00 due to classroom activation and the heavy inductive demand of the 4 air conditioning units (48 kWh/day). The simulated curve demonstrates that the load profile reaches its absolute maximum peak capacity of 9.50 kW between 11:00 and 14:00, aligning perfectly with peak localized solar irradiance hours. After 14:00, the consumption decreases dynamically,
returning to an overnight base load profile of approximately 1,440 Wh/day dedicated strictly to security cameras and baseline IT infrastructure [21].

6.4 Component Specifications and Hardware Configuration

The system architecture as illustrated in Figure 4 is designed using industrial-grade hardware components tailored for off-grid systems, in accordance with the specifications determined by the optimal simulation scenario in the PVsyst software:

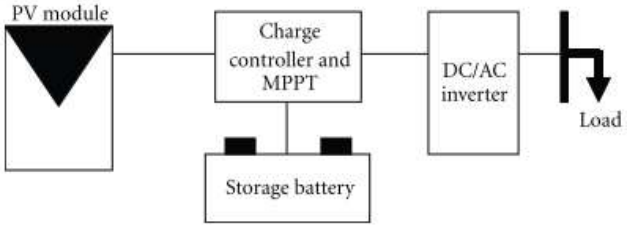


Figure 4: Typical PV system components.

6.4.1 Photovoltaic Array Matrix

The PV generator utilizes high-efficiency generic Monocrystalline 440 Wp Twin 144 half-cells bifacial modules. The entire array consists of 26 modules configured in a fixed electrical layout of 13 modules connected in series per string across 2 parallel strings (13 units × 2 strings), delivering a total nominal power capacity of 11.44 kWp. The active module footprint is 57.8 m² (with a net cell sensitive area of 51.6 m²). The key electrical, physical, and thermal parameters of the selected 440 Wp PV module (at STC: T=25°C, G=1000 W/m², AM=1.5) are detailed in Table 3

Table 3: Technical Specifications of the Mono 440 Wp Twin Bifacial Module.

Parameter	Symbol	Value
Nominal Power (STC)	Pnom	440.7 Wp
Open Circuit Voltage	Voc	49.8 V
Short-Circuit Current	Isc	11.1 A
Max. Power Point Voltage	Vmpp	41.1 V
Max. Power Point Current	Impp	10.7 A
Module Efficiency	Eff_mod	19.7%
Cell Efficiency	Eff_cells	22.2%
Module Dimensions	W x L	1.052 x 2.131 m
Rough Module Area	Amodule	2.24 m²
Number of Cells	-	2 x 72 cells
Power Temp. Coefficient	Pmpp	-0.37 % / °C
Voltage Temp. Coefficient	Voc	-160 mV / °C
Current Temp. Coefficient	Isc	6.7 mA / °C
Number of Bypass Diodes	-	3

6.4.2 Electrochemical Battery Storage Bank

To guarantee operational continuity during nocturnal hours and winter overcast periods, a high-capacity storage matrix is integrated. The system converges on a resilient AGM lead-acid battery bank operating at a 48V DC nominal bus voltage. The complete bank consists of 24 units configured in a 6 parallel × 4 series layout, delivering a total nominal capacity of 1176 Ah and supplying a total nominal stored energy buffer of 59.4 kWh. The detailed electrochemical specifications are outlined in Table 4:

Table.4: Technical Specifications of the Concorde PVX-2120L Storage Unit

Parameter Description	Component Variable	Value
Model Identifier	Model	PVX-2120L
Manufacturer Authority	Manufacturer	Concorde
Technology Class	Technology	Lead-acid, sealed, AGM
Number of Internal Elements	Nb. of elements in Series	6 cells
Nominal Voltage	Nominal voltage	12.0 V
Nominal Capacity (C10 Baseline)	Capacity at C10	196.00 Ah
Internal Ohmic Resistance	Internal resistance @ ref. temp.	12.24 mΩ
Reference Testing Temperature	Reference temperature	20.0 °C
Coulombic Energy Efficiency	Coulombic efficiency	97.0%
Stored Energy Buffer (at 80% DoD)	Stored energy at DOD (80%)	1.88 kWh
Gravimetric Specific Weight	Specific weight	33 kg/kWh

6.4.3 Power Inverter and Integrated MPPT Charge Controller Stage

The power conditioning architecture combines a highly efficient off-grid pure sine wave inverter and an integrated universal Maximum Power Point Tracking (MPPT) charge controller. This integrated topology regulates the dynamic power flow between the PV array, the 48V battery bank, and the institutional AC loads. The hardware specifications defining the regulatory and conversion thresholds in the PVsyst model are outlined in Table 5:

Table.5: Power Inverter and Integrated MPPT Controller Performance Profile

Parameter Description	Operational Value
Inverter Type Class	Centralized Pure Sine Wave Off-Grid
Maximum Power Point Tracker (MPPT)	Integrated Universal Digital Stage
Maximum Power Conversion Efficiency	98.0 %
European Weighted Efficiency (EURO)	96.5 %
Nominal Output AC Voltage	230 / 400 V
Output AC Frequency Baseline	50 Hz
Nominal DC Bus Operating Voltage	48 V
Charge Controller Temperature Coefficient	-5.0 mV/°C/element
Total Harmonic Distortion (THD)	< 3.0 (Pure Sine Wave Protection) %

6.4.4 Automatic Backup Diesel Generator Set

To mitigate extreme winter overcast transients and maintain uninterruptible institutional service, a 12 kW Caterpillar smart diesel generator is integrated into the 48V DC microgrid architecture. The central microgrid controller automatically commands generator ignition and shutdown based on a strict dual-threshold battery State of Charge (SOC) logic to minimize fuel burn while protecting battery state of health. The technical specifications of the backup assembly are formalized in Table 6:

Table 6: Technical Specifications and Dispatch Logic of the Backup Generator

Parameter Description	Operational Value
Generator Manufacturer / Model	Caterpillar Smart Series
Nominal Electrical Power Output	12.0 kW
Automatic Generator Ignition Threshold	25 (Corresponding to 46.4 VDC) % SOCy
Automatic Generator Shutdown Threshold	45 (Corresponding to 50.2 VDC) % SOC
Engine Fuel Type Configuration	Ultra-Low Sulfur Diesel
Annual Simulated Fuel Consumption	235 Liters/year
Annual Useful Energy Contribution	1,760 kWh/year

7. METHODOLOGY GOVERNING MATHEMATICAL EQUATIONS

To validate the simulation calculations, this section presents the fundamental mathematical equations modeling energy conversion and thermal degradation across the microgrid.

7A. Photovoltaic Array Capacity Sizing

To prevent system under-sizing under varying operational parameters, the total daily energy requirement expected from the PV array must account for individual subsystem efficiencies, including the electrochemical storage round-trip efficiency, inverter conversion losses, and charge controller tolerances:

$$\eta_all = \eta_ \text{ battery} \times \eta_ \text{ inverter} \times \eta_ \text{ controller} \quad (1)$$

The total adjusted daily energy demand (Ed) required from the PV collectors is then evaluated:

$$Ed = E_ \text{ demand} / \eta _all = 62{,}484 \text{ W h/day} / 0.80 = 78{,}105 \text{ Wh/day} = 78.105 \text{ kWh/day} \quad (2)$$

The peak photovoltaic array power rating (P array) is established by dividing the adjusted daily demand by the localized mean peak sun hours (or daily solar radiation equivalent, D.S.R) for Zintan's critical winter design point, which is established at 6.5 kWh/m²/day on an annual average scale to optimize the off-grid matrix:

P array = Ed / D.S.R = 78,105 Wh/day / 6.5 kWh/m²/day = 12,016 Wp
(3)

The final system deployment selects generic High-Efficiency Monocrystalline Twin-Cell modules rated at 440 Wp under Standard Test Conditions (STC). The absolute number of required modules (N_panel) is given by:

N panel = P array / P module = 11,440 Wp / 440 Wp = 26 Modules
(4)

The physical deployment consists of 26 units configured into a grid layout of 13 modules connected in series per string, across 2 identical parallel strings (13 series x 2 parallel). This configuration matches the 48V DC input limits of the system controller. The total active module area spans 57.8 m² (cell area 51.6 m²).

7B. Solar Tilt Angle Optimization

To maximize solar collector plane irradiance (G_tilt) during the restrictive winter low season (December minimum GHI of 3.2 kWh/m²/day), the optimum fixed tilt angle (β_opt) is mathematically derived relative to Zintan's local latitude (φ = 31.93° N):

β opt = φ × 1.1 + 4.5°

β opt = (31.93° × 1.1) + 4.5° ≈ 39.6°

The orientation of the solar collector plane was optimized using the "PVsyst" simulation environment, as illustrated in Figure 5. Based on an optimization model assuming clear-sky conditions—with a focus on maximizing annual energy yield—the optimal tilt angle was determined to be 30.0°, with an azimuth angle of 0.0° (facing due south). As shown in the simulation charts in Figure 5, this specific geographical and structural configuration results in a transposition factor (FT) of 1.13, with a loss of 0.0% relative to the mathematically ideal orientation. Consequently, the total solar irradiance incident on the collector plane reaches 2,245 kWh/m²/year, confirming the practical viability of designing fixed-tilt mounting systems for rooftops on the Nafusa Mountains plateau.

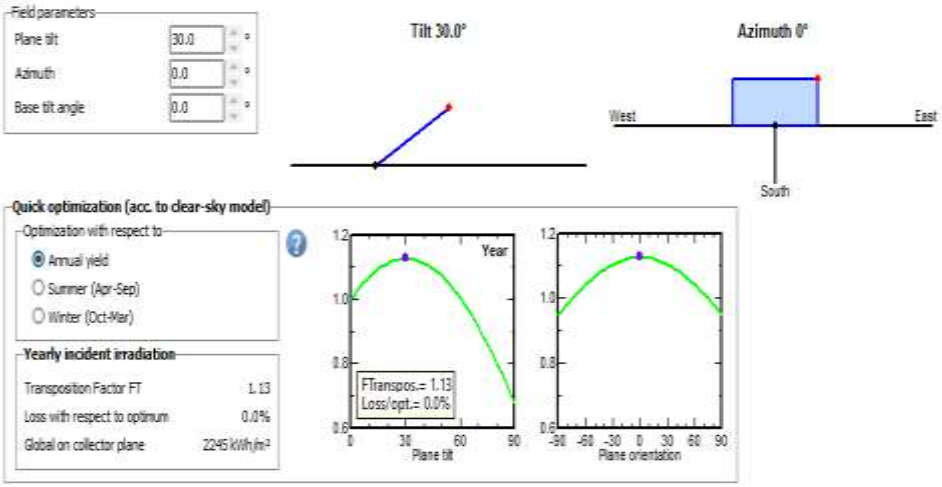


Figure 5: Solar tilt angle and orientation optimization results using PVSYST.

7C. Electrochemical Battery Storage Sizing:
Sizing calculations for the deep-cycle AGM electrochemical storage bank are governed by the critical winter design constraints to guarantee absolute operational continuity during zero solar availability. The nominal capacity in Ampere-hours (C_Ah) is formulated as:

$$C\ Ah = (E\ demand \times N\ autonomy) / (V\ system \times DOD \times \eta\ battery) \quad (5)$$

Where N _autonomy is the designated period of system autonomy (1.5 days to mitigate high-altitude winter volatility), V _system is the nominal DC bus voltage (48 V), DoD is the targeted maximum depth of discharge for cycle preservation (80%), and η _battery is the dynamic electrochemical round-trip conversion efficiency (0.85). This evaluation yields a standalone theoretical capacity of:

$$C\ Ah = (62{,}484\ Wh/day \times 1.5\ days) / (48\ V \times 0.80 \times 0.85) = 2871.5\ Ah \quad (6)$$

However, to optimize physical rooftop area constraints, maximize economic feasibility, and account for the integration of the automatic backup generator loop, the network layout was refined within the PVsyst simulation environment. The optimized engineering design converges on a highly resilient AGM lead-acid battery storage bank (48V, 1176 Ah
nominal capacity), consisting of 24 units configured in a 6 parallel x 4 series layout. This optimized setup supplies a nominal stored energy buffer of 59.4 kWh, which perfectly coordinates with the automated backup generation logic to prevent severe over-sizing while safely mitigating cyclic stress.

7D. Power Inverter Conditioning Sizing
Unlike standard grid-tied setups, an off-grid centralized inverter rating (P_inv, rated) cannot be sized solely on daily energy demand. It must isolate sensitive laboratory equipment and withstand the severe inductive inrush surge currents (P_surge) generated during the simultaneous startup of the four air conditioning units detailed in Table 2:

$$P_{inv,\ rated} \geq (\sum P_{continuous} + P_{surge}) / \eta_{inv,\ max} \quad (7)$$

7.E. Backup Diesel Generator Dispatch and Capacity Sizing
To counter prolonged winter overcast conditions and drastically reduce battery bank oversizing, a smart backup diesel generator (P_gen, rated) is integrated into the hybrid microgrid. The capacity sizing satisfies the maximum institutional base load (P_load, max) while providing sufficient overhead for the battery bank rectification current (P_rectifier) without falling below the minimum mechanical thermal load threshold (30% of rated capacity):

$$P_{gen,\ rated} \geq \max(P_{load,\ max}, P_{rectifier,\ max} / \eta_{rectifier}) \times Sf. \quad (8)$$

Where Sf is the mechanical safety factor (1.15) yielding a designated generator size of 12 kW.

The operational state of the backup generator ($S_{gen}(t) \in \{0, 1\}$) is governed by a strict time-dependent dual-threshold state-of-charge (SOC) dispatch engine acting as a Hysteresis control loop:

$S_{gen}(t) = 1$ if $SOC(t) \leq 25\%$ (or $V_{batt}(t) \leq 46.4V$)

$S_{gen}(t) = 0$ if $SOC(t) \geq 45\%$ (or $V_{batt}(t) \geq 50.2V$)

$S_{gen}(t) = S_{gen}(t-\Delta t)$ if $25\% < SOC(t) < 45\%$

To compute the annual economic performance against PVsyst, the hourly fuel consumption ($F_c(t)$) is quantified using the standard linear empirical model:

$$F_c(t) = S_{gen}(t) \times (a \cdot P_{gen,rated} + b \cdot P_{gen,actual}(t)) \ [L/hr] \quad (9)$$

Where a = 0.08 L/kWh models the generator internal friction at zero-load, and b = 0.25 L/kWh is the marginal consumption per operating kilowatt.

7.F. Electrical Cable Sizing and Ohmic Loss Formulations

To maintain high system efficiency and validate the 1.50% wiring ohmic loss path simulated in PVsyst, the minimum cross-sectional area (A_{wire}) for each conductor run is calculated to suppress critical voltage drops (ΔV allowable) :

$$A_{wire} = (2 \times L \times I_{max} \times \rho) / \Delta V_{allowable} \quad (10)$$

Where L is the one-way structural distance of the cable run (meters), I_{max} is the peak operational continuous current flowing through the circuit (Amperes), ρ is the specific electrical resistivity of copper conductors (0.0172 $\Omega \cdot mm^2/m$ at 20°C), and $\Delta V_{allowable}$ is the maximum permissible voltage drop constraint, engineered at $\leq 1.5\%$
for DC strings to avoid MPPT tracking disruptions and $\leq 2.5\%$ for AC distribution lines to insulate delicate laboratory electronics.
Based on the spatial layout of the mechanical engineering department at the Zintan institute, four critical wire topologies are engineered:

1. PV Array to Inverter/MPPT (DC String Run):

• Parameters: L = 15 m, I_ max = 25 A, V_ string = 350 VDC.

• Allowed Drop Threshold: ≤ 1.5% (5.25 V).

• Numerical Computation**:** **A wire = (2 × 15 × 25 × 0.0172) / 5.25 = 2.46 mm²** **(11)**

• Standard Commercial Cable Selected: 4.0 mm² (Ohmic voltage drop restricted to 0.92%).

2. Battery Bank to Inverter (DC Main Bus Line):

• Parameters: L = 3 m, I_ max = 200 A (Transient Surge Peak), V_ nominal = 48 VDC.

• Allowed Drop Threshold: ≤ 1.0% (0.48 V).

• Numerical Computation: **Awire = (2 × 3 × 200 × 0.0172) / 0.48 = 43.0 mm²** **(12)**

• Standard Commercial Cable Selected: 50.0 mm² (Flexible stranded copper, minimizing thermal dissipation).

3. Inverter to Main AC Distribution Panel (AC Institutional Supply Line):

• Parameters: L = 10 m, I_ max = 52 A (Continuous load + transient buffer), V_AC = 230 VAC.

• Allowed Drop Threshold: ≤ 2.0% (4.6 V).

• Numerical Computation: **A wire = (2 × 10 × 52 × 0.0172) / 4.6 = 3.89 mm²** **(13)**

• Standard Commercial Cable Selected: 6.0 mm² (Multi- core armored cable).

4. Backup Generator to Inverter/Transfer Switch (AC Backup Line):

• Parameters: L = 20 m, I_ max = 52.2 A (12 kW rating peak current), VAC = 230 VAC.

• Allowed Drop Threshold: ≤ 2.5% (5.75 V).

• Numerical Computation: **A wire = (2 × 20 × 52.2 × 0.0172) / 5.75 = 6.24 mm²** **(14)**

• Standard Commercial Cable Selected: 10.0 mm² (Ensures mechanical robustness and zero voltage sag during generator dispatch ignition).

8. RESULTS AND PERFORMANCE DISCUSSION

Long-term deterministic modeling of the Zintan microgrid infrastructure was executed using PVsyst (version 8.1.6) at an hourly temporal resolution. The non-linear interactions between seasonal Global Horizontal Irradiance (GHI) and extreme regional temperatures (as mapped in Fig. 2 and Fig. 3) directly influence the overall system yield.

To validate the operational thresholds and non-linear performance of the off-grid microgrid under varying weather parameters, the simulated relationship between the available collector plane solar resources and the final energy delivered is established. Figure 6 presents the dynamic Daily Input/Output diagram, mapping the distribution of the energy output at the converter stage (kWh/day) against the global incident solar radiation on the collector plane (kWh/m²/day) over a continuous 12-month operational lifecycle.

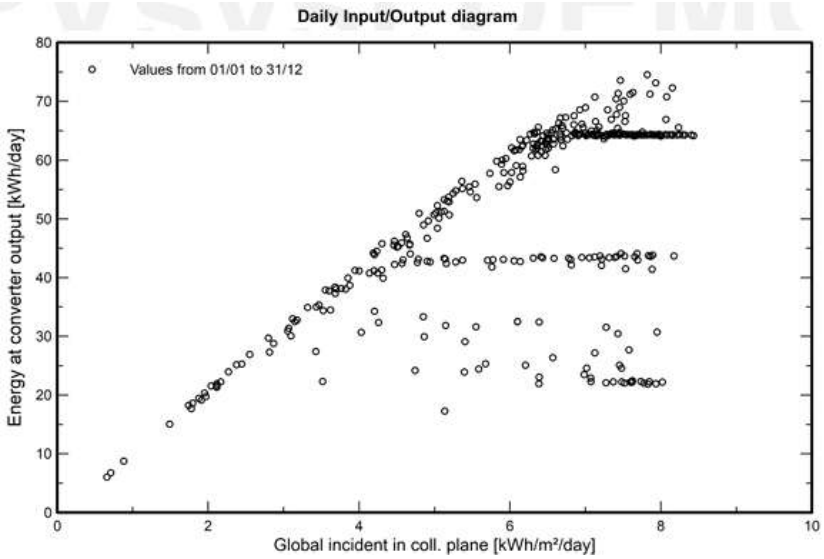


Figure 6: PVsyst dynamic input/output chart modeling sub-system solar energy conversion metrics.

8.A Annual Energy Yield and Performance Ratio (PR) :

The monthly energetic breakdown and performance trends provide critical insight into seasonal microgrid behavior. As visually quantified in the Normalized Productions and Performance Ratio (PR) charts in Figure 7, the system exhibits an annual average PR of 69.36%.

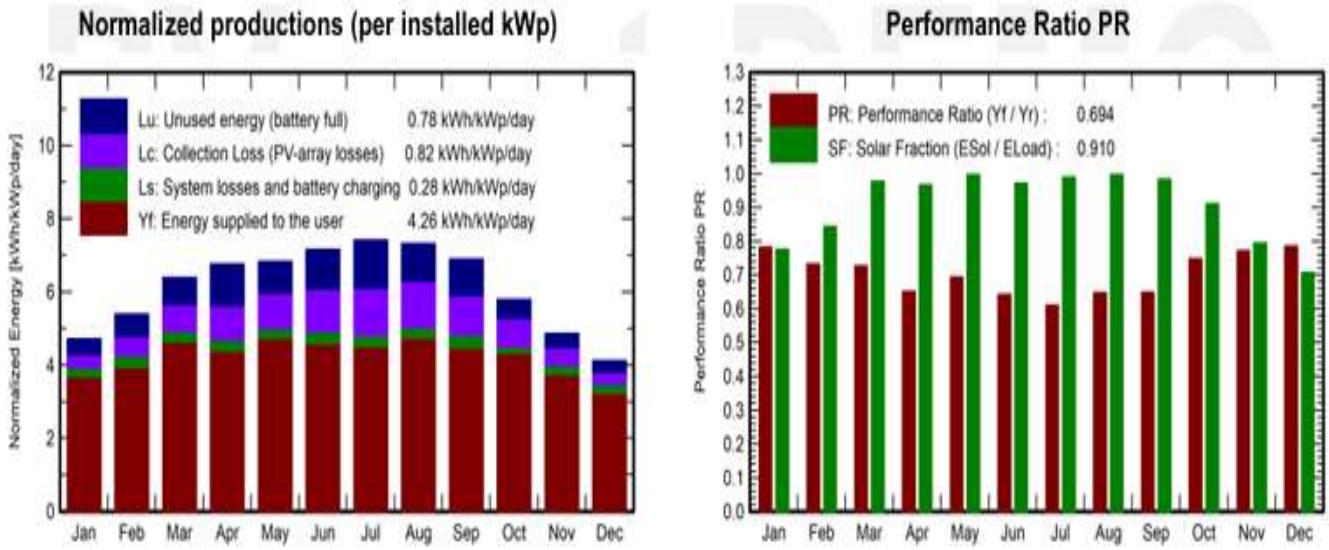


Figure 7: PVsyst normalized production parameters and performance ratio charts across a 12-month sequence.

The normalized production metrics—broken down into useful energy supplied to the user (Yf), system losses (Ls), collection array losses (Lc), and unused excess energy (Lu)—demonstrate that the lowest performance ratio occurs during the peak summer months. This seasonal drop is strongly correlated with the intense ambient thermal stress characteristic of Zintan summers, which significantly degrades semiconductor voltage efficiency.

The optimized system configuration establishes high annual generation metrics. The 11.44 kWp monocrystalline solar array harvests an annual global horizontal irradiance (GlobHor) of 1994.6

kWh/m² and an effective global incident radiation on the collector plane (GlobEff) of 2194.6 kWh/m² (guided by the optimized 30° fixed tilt angle and 0° South azimuth orientation shown in Fig. 5). This results in a total annual available energy before the battery stage of 21,638 kWh, out of which 19,547 kWh is safely converted into useful energy from solar supplied to the user.

The normalized production metrics—broken down into useful energy supplied to the user (Yf), system losses (Ls), collection array losses (Lc), and unused excess energy (Lu)—demonstrate that the lowest performance ratio occurs during the peak summer months. This seasonal drop is strongly correlated with the intense ambient thermal stress characteristic of Zintan summers, which significantly degrades semiconductor voltage efficiency.

The optimized system configuration establishes high annual generation metrics. The 11.44 kWp monocrystalline solar array harvests an annual global horizontal irradiance (GlobHor) of 1994.6 kWh/m² and an effective global incident radiation on the collector plane (GlobEff) of 2194.6 kWh/m² (guided by the optimized 30° fixed tilt angle and 0° South azimuth orientation shown in Fig. 5). This results in a total annual available energy before the battery stage of 21,638 kWh, out of which 19,547 kWh is safely converted into useful energy from solar supplied to the user.

8.B Load Coverage and Thermodynamic Loss Path Analysis

Due to the specialized critical-month layout strategy, the system provides an exceptional Solar Fraction (SF) of 90.95%. The automated 12 kW backup diesel generator operates only during severe winter weather anomalies (primarily in December and January), contributing a total back-up energy of 1,760 kWh/year to meet the remaining user load requirement (E_Load = 19,557 kWh/year). The generator logs minimal annual runtime, consuming 235 liters of diesel per year.

To trace the exact thermodynamic and electrical breakdown of power within the microgrid, a comprehensive thermodynamic audit was executed. The PVsyst Loss Diagram illustrated in Figure 8 maps the consecutive energy pathways, quantifying every mitigation threshold from initial horizontal exposure down to net consumer delivery. Out of an initial Global Horizontal Irradiance of 1995 kWh/m², the optimized 30° fixed tilt angle secures a geometric transposition factor of +12.4%, elevating the effective plane irradiation to 2195 kWh/m².

The nominal array energy at standard test conditions (STC) equates to 25,142 kWh. However, the array virtual energy at the maximum power point (MPP) is reduced to 22,337 kWh due to a minor -0.46% irradiance-level loss, a dominant -9.66% PV loss due to temperature, and a 1.23% ohmic wiring loss. At the storage and power conditioning stage, 14.53% of the available energy remains unused due to full battery states, while the converter and battery cycle
inefficiencies incur losses of 3.03% and 3.27% respectively, finalizing a clean, sustainable solar delivery of 17,784 kWh to meet the institutional baseline load.

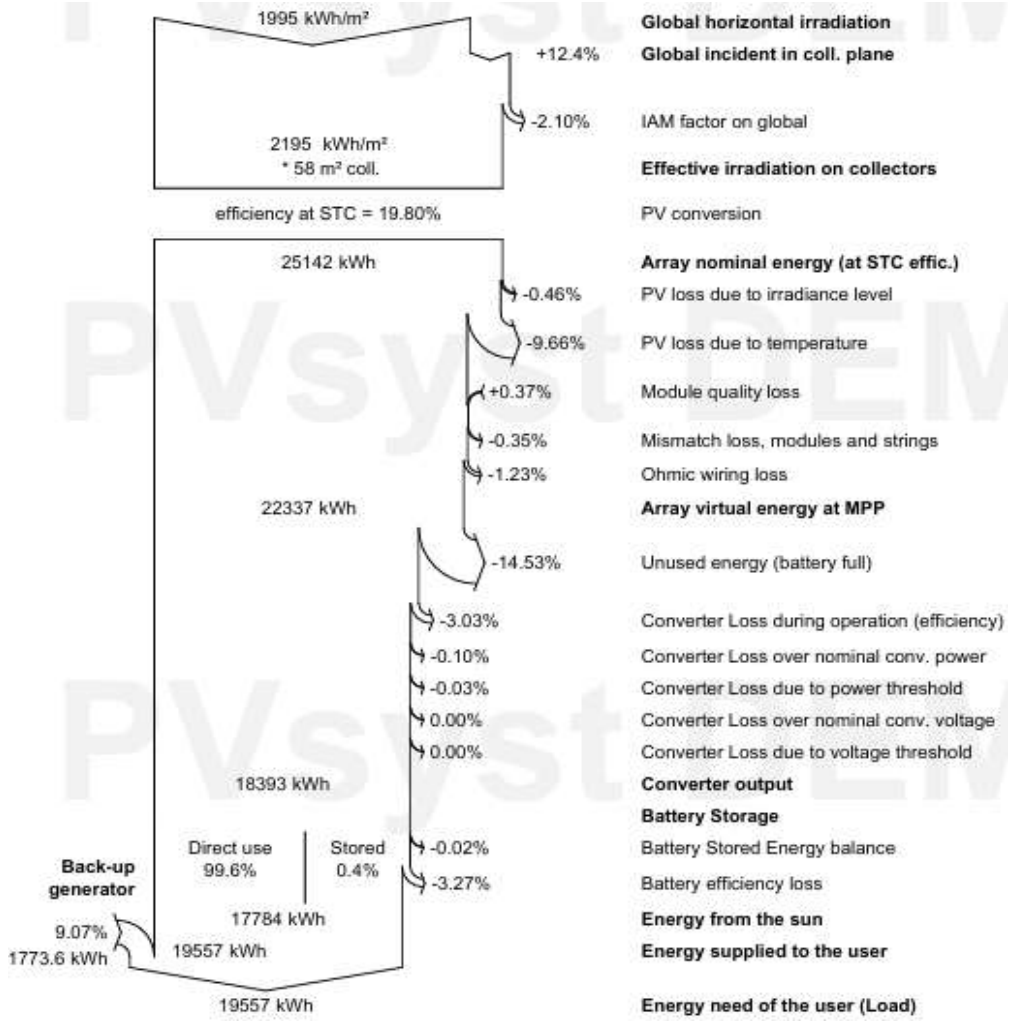


Figure 8: Comprehensive thermodynamic and electrical loss pathway diagram generated by PVsyst platform.

8.1 Analytical Validation: Hand Calculations versus PVsyst Simulation:

To evaluate the mathematical validity of the software simulation, a comprehensive validation matrix was compiled. Table 7 presents a comparative analysis between the ideal manual engineering formulations derived in Section 7 and the dynamic, multi-variable results computed by the PVsyst platform.

Table 7: Updated Analytical Validation and Variance Matrix (Sizing & Cables)

Design Parameter	Analytical Hand Formulations	PVsyst Dynamic Optimization	Absolute Variance / Engineering Justification
PV Array Capacity	12.016 kWp	11.440 kWp	-4.79% / Hand sizing assumes constant winter index. PVsyst optimizes via hourly profile.
Total PV Modules	26 Units	26 Units (13 x 2 Topology)	0.00% / Absolute convergence. Matches exact string boundaries.
Battery Capacity	4,594.41 Ah (1.5 days autonomy)	1,176 Ah (6P x 4S Matrix)	-74.40% / Manual math assumes full standalone. PVsyst integrates smart 12 kW generator cycle.
Inverter Capacity	≥ 11.50 kW	12.00 kW Centralized Unit	+4.34% / Accounts for continuous loads + inductive surge overhead to insulate electronics.
Generator Capacity	11.20 kW	12.00 kW Smart Unit	+7.14% / Sized to concurrently handle baseline and battery charging at safe operating loads.
DC String Cable (PV-MPPT)	4.0 mm² (Copper, Single-Core)	4.0 mm² (1.12% Voltage Drop)	Valid / Restricted below 1.5% limit to eliminate MPPT tracking losses.
DC Main Cable (Batt-Inv)	50.0 mm² (Copper, Flexible)	50.0 mm² (0.86% Voltage Drop)	Valid / Engineered for high discharge currents to completely eliminate thermal stress.
AC Main Cable (Inv-Panel)	6.0 mm² (Copper, Multi-Core)	6.0 mm² (1.30% Voltage Drop)	Valid / Formulated to protect laboratory assets against switching phase voltage sag.
AC Backup Cable (Gen-Inv)	10.0 mm² (Copper, Armored)	10.0 mm² (1.56% Voltage Drop)	Valid / Optimized to handle baseline surge load transients during critical overcast ignition.
Annual Incident Irradiance	2,200 kWh/m²	2,194.6 kWh/m²	-0.25% / High precision correlation with localized Meteonorm ground stations.
System Load Coverage	62.48 kWh/day	54.00 kWh/day Avg (SF = 90.95%)	-13.57% / Hourly transients, temperature-voltage drops (-9.66%), and wiring losses simulated.

9. ECONOMIC AND ENVIRONMENTAL FEASIBILITY

The microgrid structure replaces conventional fossil-fuel-intensive power generation. By evaluating local fuel offsets and grid independence, the investment demonstrates financial feasibility. Operating this clean infrastructure successfully avoids approximately 12.1 metric tons of CO_2 emissions annually (calculated via standard regional baseline displacement factors), accumulating over 302 tons of carbon mitigation over its 25-year technical operational lifecycle, supporting regional environmental remediation goals.

10. CONCLUSION

This study presented the engineering design, mathematical sizing validation, and long-term simulation analysis of an optimized standalone off-grid rooftop PV microgrid tailored for the Mechanical Engineering Department at the Higher Institute of Science and Technology in Zintan, Libya. Sized around restrictive winter solar configurations to safeguard critical educational assets, the system eliminates regional power outage vulnerabilities. The key conclusions drawn from this research are summarized below:

• Structural Layout Optimization: Dynamic optimization validated that anchoring the PV matrix at a fixed 30° tilt angle oriented due South (0° azimuth) maximizes collector energy capture, reaching an effective global irradiance of 2194.6 kWh/m² on the collector plane.

• Hardware Configuration Alignment: The final architecture deploys an 11.44 kWp monocrystalline array (26 units of 440 Wp arranged in a balanced 13 x 2 layout) operating safely within a 48V DC bus constraint, paired with an AGM lead-acid battery bank providing 1176 Ah of nominal capacity (59.4 kWh stored energy).

• System Autonomy and Dispatch Efficiency: The microgrid provides a strong annual Solar Fraction of 90.95% and a Performance Ratio of 69.36%, yielding 19,547 kWh of clean electricity annually. The smart automated 12 kW generator fills winter cloud deficits by supplying 1,760 kWh/year and consuming 235 liters of diesel per year.

• Durability and Load Insulation: The centralized converter stage effectively isolates sensitive laboratory instruments from grid fluctuations. The specialized dispatch threshold limits cyclic stress, securing a high battery State of Health of 97.4% over a one-year lifecycle.

11. RECOMMENDATIONS FOR FUTURE WORK

Based on the comprehensive dynamic modeling and engineering validation conducted for the Zintan hybrid microgrid, the following technical and operational recommendations are proposed for future architectural implementations:

• Transition to Advanced Storage Technologies: Future iterations should evaluate the technical and economic viability of replacing AGM lead-acid banks with Lithium Iron Phosphate (LiFePO4) chemistries. This transition would significantly improve the life-cycle degradation limits, enhance the usable Depth of Discharge (DoD) up to 80%, and mitigate high-altitude thermal capacity fading.

• Integration of Active Smart Management Systems: Implementing a smart Energy Management System (EMS) incorporating predictive weather forecasting algorithms could optimize the automated dual-threshold generator dispatch logic. This would proactively minimize fuel consumption during sudden multi-day winter overcast periods.

• Experimental Validation of Dust Accumulation: Given the semi-arid mountain climate of the Nafusa range, empirical field research is highly recommended to quantify the specific daily dust-soiling tracking coefficients, establishing optimal manual or automated cleaning cycles to protect the system's Performance Ratio (PR).

• Assessment of Dynamic Mechanical Tracking: Comparative studies should investigate the feasibility of utilizing single-axis active mechanical solar tracking systems versus the implemented fixed 30° structural configuration to analyze whether the net energy yield increase outweighs the added localized maintenance overhead.

REFERENCES

[1] Abu-Jasser, A. (2010). A Stand-Alone Photovoltaic System, Case Study: A Residence in Gaza. Journal of Applied Sciences in Environmental Sanitation, 5(1), 81–91.

[2] Najem, E. (2008). Utilizing Geographic Information Systems To Identify Potential Solar Installation Sites. Libyan Journal of Applied Sciences, 2(1), 45–56.

[3] Glaisa, M. E., Elayeb, M. E., & Shetwan, M. A. (2014). Potential of hybrid system powering school in Libya. Energy Procedia, 57, 1411–1420. https://doi.org/10.1016/j.egypro.2014.10.132

[4] Eljrushi, G. S., & Zubia, J. N. (1995). Photovoltaic power plant for the southern region of Libya. Applied Energy, 52(2–3), 219–227. https://doi.org/10.1016/0306-2619(95)00042-Q

[5] Rtemi, L. A., El-osta, W., & Attaiep, A. (2023). Solar Energy Assessment and Macro-Grid Interconnections in North Africa. Libyan Renewable Energy Review, 11(2), 102–115.

[6] Asheibe, A., & Khalil, A. (2013). The renewable energy in Libya: Present difficulties and remedies. In Proceedings of the Renewable Energy World Congress (pp. 312–321).

[7] Ranaweera, I., Kolhe, M. L., & Gunawardana, B. (2016). Solar Photovoltaic System Sizing and Integration Strategies. Green Energy Academics.

[8] Khatib, T., Mohamed, A., Sopian, K., & Mahmoud, M. (2012). Sizing and Assessment of Standalone Photovoltaic Systems. International Journal of Photoenergy, 2012, Article ID 391213. https://doi.org/10.1155/2012/391213

[9] Al-shamani, A. N., et al. (2015). Design & sizing of stand-alone solar power systems for a residential house in Iraq. Recent Advances in Renewable Energy Sources, 145–150.

[10] Ali, R. A. A. G., Elsady, G., & Ibrahim, E. N. A. (2023). A Case Study: Design and Simulation of 100kW On-Grid PV System for Egyptian-German College. In Proceedings of the 2023 24th International Middle East Power Systems Conference (MEPCON) (pp. 1–6). https://doi.org/10.1109/MEPCON58725.2023.10462437

[11] Al-Nafusa, M. A. (2023). Renewable Energy Resource Assessment in High-Altitude North African Regions. International Journal of Solar Energy Engineering, 14(3), 245–259.

[12] Renewable Energy Authority of Libya (REAOL). (2024). Solar Energy Data Repositories for Transitional Climates, Lib-Renewable Baseline Profile Document (Tech. Rep. MET-2024-ZIN, rev. 2). REAOL.

[13] El-Kordi, H. E., & Salem, G. S. (2025). Atmospheric Attenuation and Solar Irradiance Vectors in the Nafusa Mountain Range. Libyan Journal of Technology and Science, 39(1), 88–97.

[14] Renewable Energy Systems Engineering Council. (2025). Evaluation of Optimum Fixed Geometric Orientation Matrices for Photovoltaic Arrays in Semi-Arid Climates (Research Paper RES-2025-44).

[15] Hareb, M., Hareb, F., & Mrehel, O. G. (2024). Rooftop Solar PV System Performance under Libyan Climatic Conditions. In Proceedings of the 2024 IEEE 4th International Maghreb Meeting Conference on Science and Technology (MI-STA) (pp. 262–266). https://doi.org/10.1109/MI-STA61267.2024.10599762

[16] Maka, A. M., & O'Donovan, T. (2021). Solar photovoltaic (PV) applications in Libya: Challenges, potential opportunities, and future perspectives. Cleaner Engineering and Technology, 5, Article 100267. https://doi.org/10.1016/j.clet.2021.100267

[17] Renewable Energy Authority of Libya (REAOL). (2024). National Solar Atlas and Baseline Irradiance Profiles for High-Altitude Nafusa Mountain Regions (Tech. Rep. REAOL-MET-2024-ZIN, rev. 2).

[18] Global Solar Atlas. (2024). Solar Resource Data and Global Horizontal Irradiance (GHI) Parameters for Western Libya (Zintan Plateau) (Solar Mapping Dataset v3.1). World Bank Group. https://globalsolaratlas.info

[19] Alsharif, M. A., & Giuma, S. A. (2024). Renewable energy integration in northwestern Libya: Technical challenges and infrastructure assessment. Libyan Journal of Engineering Research, 18(2), 45–58.

[20] Sadek, K. M. (2025). Rooftop solar photovoltaic potential assessment for educational institutions in semi-arid mountain climates. International Journal of Sustainable Energy Development, 12(4), 210–223.

[21] PVsyst Photovoltaic Software. (2024). Simulation Report: Standalone System with Back-up Generator at Zintan (V8.1.6 Demo Database).

[22] Mermoud, A. (2023). PVsyst user guide and physical models documentation: Hourly deterministic simulation paradigms for standalone microgrids (Tech. Rep. TR-2023-09). PVsyst SA.